PROCEEDINGS OF SCIENCE

Higgs physics prospects at a 3 TeV muon collider

M. Casarsa,[a,*] **P. Andreetto,**[b] **L. Buonincontri,**[b,c] **L. Castelli,**[d,e] **G. Da Molin,**[f] **L. Giambastiani,**[b,c] **A. Gianelle,**[b] **K. Krizka,**[g] **D. Lucchesi,**[b,c,h] **A. Montella,**[i] **S. Pagan Griso,**[j] **L. Sestini**[b] **and D. Zuliani**[b,c]

on behalf of the International Muon Collider Collaboration

[a] *INFN Sezione di Trieste, Trieste, Italy*
[b] *INFN Sezione di Padova, Padova, Italy*
[c] *Università di Padova, Padova, Italy*
[d] *INFN Sezione di Roma, Roma, Italy*
[e] *Sapienza Università di Roma, Roma, Italy*
[f] *Laboratório de Instrumentação e Física Experimental de Partículas (LIP), Lisboa, Portugal*
[g] *University of Birmingham, Birmingham, United Kingdom*
[h] *Organisation Européenne pour la Recherche Nucléaire (CERN), Geneva, Switzerland*
[i] *Stockholm University, Stockholm, Sweden*
[j] *Lawrence Berkeley National Laboratory, Berkeley, California, USA*

E-mail: massimo.casarsa@ts.infn.it

Muon collisions at multi-TeV center-of-mass energies are an ideal environment to study the properties of the Higgs boson. The high production rates of the Higgs boson at these energies enable precise measurements of its couplings to the standard model fermions and bosons. In addition, a measurement of the double-Higgs production cross section allows to determine the trilinear self-coupling of the Higgs boson and thus to probe the Higgs field potential. This contribution presents the expected statistical sensitivities on the Higgs boson production cross sections at a 3 TeV muon collider with a dataset of 1 ab^{-1}. The results are obtained using a detailed detector simulation for the signal and physics background samples and take into account the effects of the beam-induced background on the detector performance.

The European Physical Society Conference on High Energy Physics (EPS-HEP2023)
21-25 August 2023
Hamburg, Germany

*Speaker

© Copyright owned by the author(s) under the terms of the Creative Commons Attribution-NonCommercial-NoDerivatives 4.0 International License (CC BY-NC-ND 4.0).

PoS(EPS-HEP2023)408

1. Introduction

Lepton collisions at multi-TeV center-of-mass energies provide an ideal environment to test the standard model predictions with unprecedented precision, particularly in the Higgs sector. The high production rates of the Higgs boson allow to precisely measure its couplings to fermions and bosons, and to probe the trilinear and quartic self-couplings that determine the shape of the Higgs field potential. In leptonic collisions at center-of-mass energies $\sqrt{s}$ above a few TeV, the production of the Higgs boson is mainly driven by vector boson fusion processes, which exhibit cross sections that logarithmically increase with s, as illustrated in Fig. 1.

A muon collider is the most efficient tool for producing lepton collisions at several TeV in a compact circular machine. The International Muon Collider Collaboration is developing two muon collider concepts: a 10 TeV collider that aims to achieve an integrated luminosity target of 10 ab^{-1} per interaction point over the course of 5 years, and a possible intermediate stage at 3 TeV that targets an integrated luminosity of 1 ab^{-1} per interaction point in 5 years of operation. Table 1 shows the cross sections of the primary production modes for the Higgs boson at $\sqrt{s}$ = 3 and 10 TeV, along with the Higgs boson samples that are expected in the two scenarios.

However, the unstable nature of muons poses unique challenges to the experimental apparatus, as it results in extremely high levels of machine background in the detector. The interactions between the decay products of the muons in the beams and the machine components are the main source of machine background (beam-induced background, BIB). The BIB is an unusual machine background, which is not generated by collisions at the interaction point, but is intrinsic to the muon beams [2]. Very high hit multiplicities are expected in the detector's tracking system and a uniform diffuse energy deposition in the calorimeters. Mitigation techniques and specialized algorithms for the reconstruction of physics objects are therefore required [3]. These experimental conditions are unique, making it very difficult, if not impossible, to predict their impact on detector performance based on prior experience with machine backgrounds at past and present colliders. In order to assess the impact of the beam-induced background on the detector and to better estimate the physics potential of a muon collider, a first campaign of studies was carried out based on a detailed detector simulation.

2. Experimental apparatus and physics object reconstruction

The detector model used in the studies presented here is derived from CLIC's detector concept [4], which was optimized for electron-positron collisions of up to 3 TeV. Modifications were made to the vertex detector and machine-detector interface to account for the more severe background environment of a muon collider. The detector comprises a tracking system, hermetic high-granularity electromagnetic and hadronic calorimeters, and a muon spectrometer. Both the tracking detectors and the calorimeters are immersed in a 3.57 T solenoidal magnetic field. The tracking system consists of a silicon vertex detector and inner and outer silicon trackers. The electromagnetic and hadronic calorimeters are sampling calorimeters composed of 40 tungsten absorber layers and silicon pad sensors, and 60 steel absorber layers and plastic scintillating tiles, respectively. The muon detectors cover the outermost region of the apparatus with layers of resistive plate chambers that are interleaved in the iron return yoke of the magnet. Two tungsten cones, covered in borated

PoS(EPS-HEP2023)408

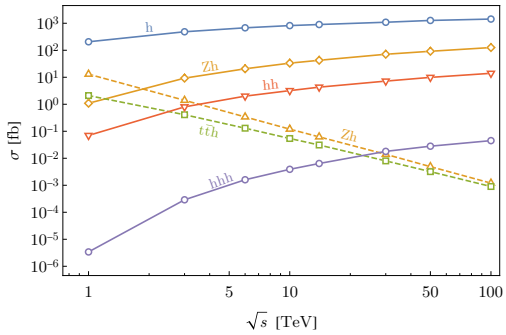

Figure 1: Cross sections for the main Higgs boson production processes as a function of the muon collider center-of-mass energy [1].

	cross section [fb]		expected events	
	3 TeV	10 TeV	1 ab^{-1} at 3 TeV	10 ab^{-1} at 10 TeV
H	550	930	5.5×10^5	9.3×10^6
ZH	11	35	1.1×10^4	3.5×10^5
$t\bar{t}H$	0.42	0.14	420	1.4×10^3
HH	0.95	3.8	950	3.8×10^4
HHH	3.0×10^{-4}	4.2×10^{-3}	0.30	42

Table 1: Cross sections for the main Higgs boson production modes at $\sqrt{s}$ = 3 and 10 TeV and the expected events in 1 ab^{-1} and 10 ab^{-1}, respectively.

polyethylene cladding and featuring an opening angle of 10°, are utilized for shielding the beampipe on both sides of the interaction region. More details can be found in Ref. [5].

The muon collider software framework [6] is based on CLIC's iLCSoft: the detector geometry is modeled with the DD4hep toolkit [7], the detector response is simulated by GEANT4 [8], and event reconstruction is done with the Marlin package [9]. The MARS15 software [10] was used to generate the beam-induced background for a collider operating at $\sqrt{s}$ = 1.5 TeV, with studies indicating that the BIB behavior at higher collision energies is mild up to 3 TeV and is not expected to significantly change the results presented here [2].

To maintain high efficiencies and resolutions for the physics objects in the presence of machine-induced background, all reconstruction algorithms required revision or fine-tuning, as described in Ref. [5]. The initial focus was on muons, photons, and jets. Muons and photons are reconstructed by the PandoraPFA algorithm [11]. The algorithm identifies muons as reconstructed trajectories (tracks) in the central tracker that match hit clusters in the muon detectors, whereas photons are identified as isolated clusters in the electromagnetic calorimeter. Hadronic jets are formed by clustering PandoraPFA objects. Corrections are applied to the reconstructed energy of photons and jets to account for detector effects and inefficiencies. Jets originating from b quarks are identified by searching for displaced secondary vertices within the jets.

3. Higgs boson production cross sections

The physics objects described in the previous section were used to reconstruct the Higgs boson decay modes into the final states $f = b\bar{b}$, WW^*, $\gamma\gamma$, ZZ^*, and $\mu^+\mu^-$ to estimate the statistical sensitivity on the production cross sections multiplied by the decay branching ratios: $\sigma_H \times BR(H \to f)$. Furthermore, the double-Higgs production HH in the $b\bar{b}b\bar{b}$ final state was also studied. The Higgs and physics background samples were generated at leading order with WHIZARD v2.8.2 [12] or MadGraph5_aMC@NLO v3.1.0 [13] and PYTHIA8 [14] was used for the hadronization of the final states. The samples were then processed with the detailed detector simulation and reconstructed with the muon collider software. All analyses share a common approach consisting of an initial loose kinematical preselection to remove the dominant backgrounds, followed by a final signal selection utilizing a multivariate analysis method. For the channels with jets in the final state, the

PoS(EPS-HEP2023)408

BIB was directly superimposed on the physics events on an event-by-event basis. For the cases with muons and photons, the analyses were performed without the BIB, whose impact was then estimated and found to be negligible. The main features of each analysis are outlined below. The results are summarized in Tab. 2. A natural reference to compare to are the corresponding results by CLIC at $\sqrt{s}$ = 3 TeV [15] with the caveat that CLIC is assuming a dataset of 2 ab^{-1} and the number of reconstructed final states for each Higgs boson decay mode are in some cases different.

$H \to b\bar{b}$: The $b\bar{b}$ channel is reconstructed with two central high-p_T jets satisfying: $p_T^{\text{jet}} > 40$ GeV and $|\eta_{\text{jet}}| < 2.5$, where $\eta_{\text{jet}} = -\log\tan(\theta_{\text{jet}}/2)$. Once the b-flavor identification is applied to both jets, the only significant backgrounds that survive are the $Z \to b\bar{b}$ and the $Z \to c\bar{c}$ processes. The number of signal and background events are estimated with a fit to the dijet mass distribution. The dijet mass resolution is critical to separate the H and Z peaks. The current value of the Higgs boson mass resolution is about 18%, being dominated by BIB effects. The estimated sensitivity on $\sigma_H \times BR(H \to b\bar{b})$ is 0.75%, to be compared with 0.3% for CLIC.

$H \to WW^*$: The WW channel is reconstructed in the semileptonic final state $q\bar{q}'\mu\nu_\mu$, which presents a favourable signal to background ratio. Events are selected with at least two reconstructed jets, having $p_T^{\text{jet}} > 20$ GeV and $|\eta_{\text{jet}}| < 2.5$, and one muon with $p_T^\mu > 10$ GeV and $10^\circ < \theta_\mu < 170^\circ$. Fake jets caused by the BIB are suppressed by requiring the number of jet constituents to be greater than two and any single constituent to carry less than 0.8 of the jet momentum. The scores of two Boosted Decision Trees (BDT), trained to distinguish signal from backgrounds with and without a Higgs boson, are used for the final signal selection. The resulting statistical uncertainty on the Higgs production cross section is 2.9%. Reconstructing the full hadronic channel and the semileptonic channels with both muons and electrons, CLIC obtains 0.7%.

$H \to \gamma\gamma$: The $\gamma\gamma$ analysis searches for events with at least two reconstructed photons, featuring $E_\gamma > 15$ GeV, $p_T^\gamma > 10$ GeV and $10^\circ < \theta_\gamma < 170^\circ$, $p_T^\gamma > 40$ GeV for the most energetic photon, and an invariant mass $m_{\gamma\gamma} > 40$ GeV. The final selection is obtained with a cut on the output of a BDT trained to separate signal events from a mixture of the background events. The reconstruction of high energy photons is not significantly affected by the BIB. In fact, the diphoton invariant mass exhibits a very good resolution of 3.2 GeV. The estimated relative uncertainty on the production cross section is 7.6%, to be compared with CLIC's 10%.

$H \to ZZ^*$: The ZZ channel is reconstructed in the semileptonic final state $q\bar{q}\mu^+\mu^-$. Events are selected with at least two reconstructed jets and two opposite-charge muons, having $p_T^{\text{jet}} > 15$ GeV and $30^\circ < \theta_{\text{jet}} < 150^\circ$, $p_T^\mu > 10$ GeV and $10^\circ < \theta_\mu < 170^\circ$. The muon is required to be isolated from the jets in the event. The presence of at least one reconstructed track is requested in the jet to remove fake jets from the BIB. For the signal selection a BDT is trained to distinguish ZZ events from the dominant background. The sensitivity estimated on the production cross section is 17%. CLIC's analysis also includes the semileptonic channel with electrons and results in a sensitivity of 3.9%.

PoS(EPS-HEP2023)408

$\sqrt{s}$ = 3 TeV, 1 ab^{-1}	channel	σ_{eff} [fb]	ϵ_{sel} [%]	N_{evt}	$\Delta\sigma_H/\sigma_H$ [%]
$H \to b\bar{b}$	S: $b\bar{b}$	308	19.3	59500	0.75
	B: $\mu^+\mu^- \to q_h\bar{q}_h X$ ($q_h = b, c$; $X = \nu_\mu\bar{\nu}_\mu, \mu^+\mu^-$)	584	11.2	65400	
$H \to WW^*$	S: $q\bar{q}'\mu\nu_\mu$	17.3	14.1	2430	2.9
	B: $\mu^+\mu^- \to q\bar{q}'\mu\nu_\mu$	5020	0.05	2600	
$H \to \gamma\gamma$	S: $\gamma\gamma$	0.91	43.9	396	7.6
	B: $\mu^+\mu^- \to \gamma\gamma\nu_\mu\bar{\nu}_\mu$	82.0	1.1	442	
	$\mu^+\mu^- \to \ell^+\ell^-\gamma$ ($\ell = e, \mu$)	159	0.06	31	
	$\mu^+\mu^- \to \ell^+\ell^-\gamma\gamma$ ($\ell = e, \mu$)	4.41	0.3	11	
$H \to ZZ^*$	S: $q\bar{q}\mu^+\mu^-$	0.35	15.9	55	17
	B: $\mu^+\mu^- \to q\bar{q}\mu^+\mu^-$	5.67	0.69	39	
$H \to \mu^+\mu^-$	S: $\mu^+\mu^-$	0.12	21.6	26	38
	B: $\mu^+\mu^- \to \mu^+\mu^-\nu_\mu\bar{\nu}_\mu$	11.1	5.74	637	
	$\mu^+\mu^- \to \mu^+\mu^-\mu^+\mu^-$	297.4	0.16	476	
$HH \to b\bar{b}b\bar{b}$	S: $b\bar{b}b\bar{b}$	0.28	27.5	77	33
	B: $\mu^+\mu^- \to q_h\bar{q}_h q_h\bar{q}_h X$ ($q_h = b, c$; $X = \nu_\mu\bar{\nu}_\mu, \mu^+\mu^-$)	4.1	17.7	724	
	$\mu^+\mu^- \to H(b\bar{b})q_h\bar{q}_h X$ ($q_h = b, c$; $X = \nu_\mu\bar{\nu}_\mu, \mu^+\mu^-$)	2.8	24.7	698	

Table 2: Summary of Higgs boson analyses using a detailed detector simulation at a 3 TeV muon collider with a dataset of 1 ab^{-1}. S and B denote the reconstructed Higgs boson decay channels and the main background processes producing the same experimental signatures, respectively. σ_{eff} is the effective cross section for the reconstructed final state, ϵ_{sel} is the total selection efficiency, and N_{evt} the number of selected events. The last column reports the estimated relative statistical uncertainty on the Higgs boson production cross section.

$H \to \mu^+\mu^-$: The $\mu\mu$ channel is reconstructed selecting events with two opposite-charge muons in the kinematical region $p_T^\mu > 5$ GeV and $10° < \theta_\mu < 170°$. In addition, the two muons are required to satisfy $p_T^{\mu^+} + p_T^{\mu^-} > 50$ GeV, $p_T^{\mu\mu} > 30$ GeV, and $105 < m_{\mu\mu} < 145$ GeV. For the final selection, two BDTs are trained to separate the signal from the two dominant backgrounds. The BIB impact on the reconstruction of muons is found to be negligible. A sensitivity on the production cross section of 38% is estimated. For this specific channel, CLIC's ability to veto events with electrons scattered at very low angles significantly reduces background contamination, resulting in a sensitivity of 25%.

$HH \to b\bar{b}b\bar{b}$: The HH production was studied in the hadronic final state: $HH \to b\bar{b}b\bar{b}$. Events are selected with at least four reconstructed jets having $p_T^{\text{jet}} > 20$ GeV. Jets are paired to reconstruct two H candidates in such a way that the pairs have the closest masses to the nominal Higgs boson mass. The requirement of b-tagging for at least one jet per pair suppresses most of the backgrounds with jets induced by light quarks. A cut on the output of an artificial neural network is used to select the final signal and background samples. The estimated sensitivity on the double-Higgs production cross section is 33%. Including also the decay channel $b\bar{b}WW^*$ with both the W bosons decaying hadronically, CLIC quotes a precision of 29%, when using non-polarized beams.

The observables $\sigma_H \times BR(H \to f)$ are sensitive to the Higgs boson couplings to b quarks, W and Z bosons, photons, and muons. The precision achievable on the couplings is usually estimated with a fit to the cross sections. The studies carried out so far with the detailed detector simulation do not cover all the most relevant decay modes of the Higgs boson; therefore, the coupling fit is not yet meaningful. As for $\sigma_{HH} \times BR(HH \to b\bar{b}b\bar{b})$, it represents a gateway to the determination of the Higgs boson trilinear self-coupling. From this study, a preliminary estimate of approximately 20-30% is derived for the sensitivity on the trilinear self-coupling [16].

PoS(EPS-HEP2023)408

4. Conclusion

The sensitivity on the production cross sections multiplied by the decay branching ratios for the Higgs boson modes $b\bar{b}$, WW^*, $\gamma\gamma$, ZZ^*, and $\mu^+\mu^-$ was studied at a 3 TeV muon collider with a dataset of 1 ab^{-1}. The study is based on a detailed detector simulation and includes the beam-induced background. The results indicate that the background effects on the detector response can be minimized to a degree that does not compromise the reconstruction performance of the physics objects and thus the physics reach of a muon collider.

The background mitigation measures, detector design, and reconstruction algorithms are not fully optimized at this time, and the analysis strategies employed are relatively basic. Nevertheless, this study demonstrates that a muon collider at a center-of-mass energy of 3 TeV has the potential to achieve results in the Higgs sector comparable to those of the extensively studied CLIC detector at the same collision energy.

5. Acknowledgments

This work was supported by the European Union's Horizon 2020 and Horizon Europe Research and Innovation programs through the Marie Skłodowska-Curie RISE Grant Agreement No. 101006726 and the Research Infrastructures INFRADEV Grant Agreement No. 101094300.

References

[1] H.A. Ali *et al.*, 2022 Rep. Prog. Phys. **85** 084201.

[2] D. Lucchesi *et al.*, PoS EPS-HEP2023, 630 (2024).

[3] L. Sestini *et al.*, PoS EPS-HEP2023, 552 (2024).

[4] N. Alipour Tehrani *et al.*, CLICdp-Note-2017-001 (2018).

[5] C. Accettura *et al.*, Eur. Phys. J. C **83**, 864 (2023).

[6] N. Bartosik *et al.*, Comput Softw Big Sci **5**, 21 (2021).

[7] M. Frank *et al.*, 2014 J. Phys.: Conf. Ser. **513** 022010.

[8] J. Allison *et al.*, Nucl. Instrum. Meth. A **835**, 186 (2016).

[9] F. Gaede, Nucl. Inst. Meth. A **559**, 177 (2006).

[10] N.V. Mokhov and C.C. James, Fermilab-FN-1058-APC (2018).

[11] M. Thomson, Nucl. Inst. Meth. A **611**, 25 (2009).

[12] W. Kilian, T. Ohl and J. Reuter, Eur. Phys. J. C **71**, 1742 (2011).

[13] J. Alwall *et al.*, J. High Energ. Phys. **2014**, 79 (2014).

[14] T. Sjöstrand *et al.*, Comput. Phys. Commun. **191**, 159 (2015).

[15] H. Abramowicz *et al.*, Eur. Phys. J. C **77**, 475 (2017).

[16] L. Sestini *et al.*, PoS EPS-ICHEP2022, 515 (2023).

PoS(EPS-HEP2023)408